



Published in final edited form as:

*J Neurophysiol.* 2007 September ; 98(3): 1440–1450. doi:10.1152/jn.00309.2007.

## Serotonin Concentrations in the Lumbosacral Spinal Cord of the Adult Rat Following Microinjection or Dorsal Surface Application

Michele R. Brumley, Ian D. Hentall, Alberto Pinzon, Brijesh H. Kadam, Anthony Blythe, Francisco J. Sanchez, Annette M. Taberner, and Brian R. Noga

*The Miami Project to Cure Paralysis, University of Miami Miller School of Medicine, Miami, Florida*

### Abstract

Application of neuroactive substances, including monoamines, is common in studies examining the spinal mechanisms of sensation and behavior. However, affected regions and time courses of transmitter activity are uncertain. We measured the spatial and temporal distribution of serotonin [5-hydroxytryptamine (5-HT)] in the lumbosacral spinal cord of halothane-anesthetized adult rats, following its intraspinal microinjection or surface application. Carbon fiber microelectrodes (CFMEs) were positioned at various locations in the spinal cord and oxidation currents corresponding to extracellular 5-HT were measured by fast cyclic voltammetry. Intraspinal microinjection of 5-HT (100  $\mu$ M, 1–3  $\mu$ l) produced responses that were most pronounced at CFMEs positioned  $\leq$ 800  $\mu$ m from the drug micropipette: 5-HT concentration was significantly higher (1.43 vs.  $<$ 0.28% of initial concentration) and response latency was shorter (67.1 vs. 598.2 s) compared with more distantly positioned CFMEs. Treatment with the selective 5-HT reuptake inhibitor clomipramine only slightly affected the spread of microinjected 5-HT. Surface application over several segments led to a transient rise in concentration that was usually apparent within 30 s and was dramatically attenuated with increasing depth: 0.25% of initial concentration (1 mM) within 400  $\mu$ m of the dorsal surface and  $<$ 0.001% between 1,170 and 2,000  $\mu$ m. This initial response to superfusion was sometimes followed by a gradual increase to a new concentration plateau. In sum, compared with bath application, microinjection can deliver about tenfold higher transmitter concentrations, but to much more restricted areas of the spinal cord.

### INTRODUCTION

Serotonin [5-hydroxytryptamine (5-HT)] is critically involved in many spinal-mediated processes, including locomotion (Barbeau and Rossignol 1991; Schmidt and Jordan 2000) and nociception (Willis and Westlund 1997) and is often applied locally to study the neural mechanisms generating these responses (e.g., Bardin et al. 1997; Kiehn and Kjærulff 1996; Lopez-Garcia 1998). Its potential use in the recovery of mobility and reduction of pain after spinal cord injury (SCI) has also been examined (Antri et al. 2002; Fong et al. 2005; Hains et al. 2001).

In experiments designed to examine the effect of 5-HT on spinal function, the dose used is judged empirically on the basis of the response. Often the assumption is made that the effects are due to specific ligand–receptor interactions, but the concentrations achieved intraspinally for a given administered concentration remain unknown. Recent work in brain and spinal cord (Šimonová et al. 1996; Syková et al. 1994) has demonstrated heterogeneity in the diffusion

Address for reprint requests and other correspondence: B. R. Noga, The Miami Project to Cure Paralysis, University of Miami Miller School of Medicine, 1095 NW 14th Terrace, Miami, FL 33136 (E-mail: bnoga@miami.edu).

Present addresses: A. Pinzon, Albert Einstein College of Medicine, Yeshiva University, Department of Neurology, New York NY 10461; B. H. Kadam, Department of Pediatrics, Marshfield Center, Marshfield, WI 54449.

and clearance of neurotransmitters. Thus the dose–response relationship may not necessarily reflect the effective concentration of the neurotransmitter in different areas of the cord, nor will it indicate accurately the time course of effects in these areas. Several considerations likely exist that affect these parameters, including the method of drug administration, site of application relative to the location of receptors mediating the effect of interest, and efficiency of extracellular clearance mechanisms. These considerations have important consequences for the interpretation of studies using drugs/transmitters to facilitate locomotion or to attenuate pain, as well as for the design of pharmacotherapeutic strategies to treat SCI.

Using carbon fiber microelectrodes (CFMEs) to oxidize substances at their surface, fast cyclic voltammetry (FCV) can measure rapid changes in extracellular monoamine levels in neural tissue, including 5-HT (Stamford et al. 1992). Thus FCV can provide the high spatial and temporal resolution needed to study the spread of 5-HT in the spinal cord (Hentall et al. 2006; Noga et al. 2004) after exogenous application.

Based on our prior work mapping brain stem–evoked monoamine release within specific laminae (Hentall et al. 2003, 2006), we formed the hypothesis that extracellularly released monoamines do not spread much beyond a few hundred microns. Here we test this hypothesis by measuring the spatiotemporal spread of 5-HT in the lumbosacral spinal cord of the adult rat using two different drug application methods—intraspinal microinjection and dorsal surface application. In the microinjection protocol, multiple CFMEs measured the spread of 5-HT only in the rostral–caudal direction after it was delivered into a focal area of the cord. Based on previously published work on diffusion characteristics within the spinal cord (Prokopová et al. 1997; Šimonová et al. 1996), we assumed that the spread of 5-HT from a point source was essentially the same in all directions. In the bath superfusion protocol, CFMEs were positioned at different depths but at a similar medial–lateral and rostral–caudal position in each experiment so that they would measure the dorsal–ventral spread of a continuous supply of 5-HT after it was rapidly applied to the dorsal surface of the cord. Although higher concentrations of 5-HT can be expected to be reached sooner at CFMEs located closer to the area of drug application, due to well-established rules of physical diffusion and biological clearance (including cellular reuptake), the degree of attenuation and delay can be ascertained only empirically. Thus we investigated the role of 5-HT transporters (SERT) in clearance by measuring the spread of microinjected 5-HT after treatment with the selective reuptake inhibitor clomipramine. We predicted that clomipramine would increase the time for the 5-HT signal to decay at all measurement sites. The results imply strong initial homeostasis of 5-HT concentrations in the adult spinal cord, and have methodological implications for behavioral and other studies using intrathecal and bath application. Preliminary data have been presented (Noga et al. 2005).

## METHODS

### Animal preparation

Subjects were 14 adult Fisher-CDF female rats (Charles River Labs, Wilmington, MA) weighing about 200 g. Care and use of animals were carried out in accordance with National Institutes of Health guidelines (National Institutes of Health Publication No. 80–23; revised 1996). The number of animals used and their pain and distress were minimized.

Animals were anesthetized and prepared for spinal voltammetric recordings using procedures described previously (Noga et al. 2004). Briefly, animals were anesthetized with 1–3% halothane in a mixture of 60% nitrous oxide and 40% oxygen: first through an induction chamber, next through a facemask, and finally through an endotracheal tube. The left common carotid artery and external jugular vein were cannulated to monitor blood pressure and administer fluids, respectively. Body temperature was maintained at 37°C using feedback-

controlled heating lamps. End tidal CO<sub>2</sub>, O<sub>2</sub>, and tissue oxygenation were monitored throughout the experiment using a Datex OscarOxy multigas monitor and pulse oximeter. All values were within their respective normal physiological ranges. A laminectomy was performed over the lumbosacral spinal cord. Animals were positioned in a stereotaxic headframe and spinal cord fixation device. A bath (or pool) was created around the exposed spinal cord, formed by skin and back muscle, and covered with a layer of Reprosil (hydrophilic vinyl polysiloxane impression material; Dentsply Caulk, Milford, DE). The bath was filled with 1–2 ml of warmed 0.1 M phosphate-buffered saline (PBS) or artificial cerebrospinal fluid (aCSF), maintained at body temperature, and had a pH value of 7.4. Small holes were made in the pia where the electrodes made contact with the spinal cord. All electrodes were lowered into the L1–S2 spinal segments using micromanipulators, and voltammetric measurements were made. Anesthetic levels were adjusted to ensure the elimination of withdrawal reflexes without producing cardiac or respiratory depression.

### Fast cyclic voltammetry

CFMEs were constructed using 33- $\mu$ m-diameter carbon fiber (Textron Systems) and 0.75- to 2.0-mm-diameter borosilicate glass micropipettes (with 40–50  $\mu$ m tip diameter). CFMEs were constructed using established procedures (Armstrong-James and Millar 1984; Hentall et al. 2003, 2006; Noga et al. 2004) and electrically pretreated as described previously (Hentall et al. 2006). Arrays containing two to four CFMEs were made by cementing the electrodes together at fixed relative positions using fast-drying epoxy (J-B Kwik; J-B Weld, Sulfur Springs, TX).

FCV was carried out using a multilead voltage-clamp amplifier (Registim LLC, model VAMP-1). Two to four of these leads were connected to active CFMEs. Two other leads were connected to a carbon-based reference electrode internally filled with KCl (Dri-Ref; WPI, Sarasota, FL) and to an Ag–AgCl auxiliary electrode, which applied the clamping current. Both the reference and the auxiliary electrodes were placed adjacent to the bath covering the spinal cord. Using the common reference and auxiliary electrodes, a brief sawtooth voltage waveform input “scan” was applied in turn (multiplexed) to each active CFME input. The sawtooth had four phases: 0 to –1 V, to +1.4 V (or +1 V), to –1, to 0 V (Fig. 1A). Its slope was 200 or 400 V/s and it was applied consecutively to the  $n$  microelectrodes at 0.5-s intervals. Thus the measurement rate was every  $n \times 0.5$  s at a given CFME.

The amplifier’s output signal was proportional to the clamping current flowing through the microelectrode resulting from the electrode charging current and the redox current resulting from the oxidation and reduction of 5-HT (and clomipramine) at the tip (exposed carbon fiber) of the CFME. This is referred to as the “full” signal. To monitor 5-HT concentrations during each experiment, the output voltammogram for each CFME obtained during the first scan in a trial was stored and subtracted from subsequent output voltammograms, yielding a “subtracted voltammogram” of changes in redox or Faradaic current. All components of the voltammograms (applied voltage waveform, the full signal, and subtracted voltammograms) were captured digitally at 10 kHz.

**SIGNAL PROCESSING**—In vivo changes in electrode impedance (affecting the full signal) can result in baseline shifts in subtracted voltammograms that can obscure or mask faradaic currents and hinder identification of the measured substances. To compensate for such changes, we multiplied each full signal by a constant factor ( $P_n$ ) that normalized the measured signal to the reference full signal [ $F_0(t)$ ] at a time “ $\tau$ ” outside the oxidation/reduction regions of the transmitters of interest, where differences between the full signals are not expected. Each multiplicative factor was obtained by dividing the reference full signal at  $\tau$  [ $F_0(\tau)$ ] by the value of each subsequent full signal at  $\tau$  [i.e.,  $P_{1,2,3,\dots,n} = F_0(\tau)/F_{1,2,3,\dots,n}(\tau)$ ]. After obtaining the

multiplicative factors, each full signal was adjusted [i.e.,  $F'_{1,2,3...n}(t) = F_{1,2,3...n}(t) \times P_{1,2,3...n}$ ] and used to calculate new subtracted signals [ $S_{1,2,3...n}(t) = F'_{1,2,3...n}(t) - F_0(t)$ ]. In instances where no electrode impedance changes occurred, the multiplicative factor equaled one and no adjustments were made.  $\tau = 1.5$  ms for all figures (i.e., color representations) based on microinjection data.

After impedance correction, subtracted faradaic waveforms were low-pass filtered off-line using a simple five-point moving average implemented in Matlab (The MathWorks, Natick, MA). Within each experiment, low-pass filtering was also performed between consecutive subtracted waveforms at each scan time point. To aid in detection and identification, the newly generated subtracted signals were displayed as landscapes or raster plots (Phillips and Stamford 1999) and colorized (Michael et al. 1998) for clarity (Fig. 1).

**CALIBRATION**—CFMEs were calibrated in vitro both before and after experiments: preexperimentally with 5-HT only and postexperimentally with 5-HT and then clomipramine. CFMEs were rinsed with distilled H<sub>2</sub>O and ethanol between calibration trials. Because insertion of CFMEs into neural tissue significantly changes electrode sensitivity (Stamford et al. 1992), postexperimental calibration values were used to estimate concentrations in vivo. Successive aliquots of each substance (dissolved in vehicle solution) were added to 10 ml PBS or aCSF (pH = 7.4; purged of oxygen with nitrogen gas) to increase the concentration of the substance: 125 nM to 2  $\mu$ M of 5-HT; 125 nM to 1 mM of clomipramine. Oxidation currents were generated during the first ascending phase of the FCV scan (Fig. 1A). Oxidation currents obtained in vitro showed average peak values occurring at approximately +800 mV for 5-HT (for a scan rate of 400 V/s). Two postoxidation reduction currents were shown for 5-HT: one occurring around +55 mV and the other around -451 mV. At low concentrations, oxidation currents for clomipramine peaked at +683 mV. Clomipramine showed only one postoxidation reduction current, occurring around -416 mV. However, at high concentrations, the redox currents peaked at much higher voltages, sometimes greater than +900 and -600 mV for oxidation and reduction peaks, respectively (Fig. 1).

The sensitivities of the CFMEs for each substance were (mean  $\pm$  SE): 13.2  $\pm$  0.7 nM/nA for 5-HT and 1.1  $\pm$  0.1  $\mu$ M/nA for clomipramine. CFMEs showed a linear response to different concentrations of 5-HT (Fig. 1B). The detection threshold for 5-HT was calculated from the baseline noise, using twice the SE measured from four to nine scans (the number of scans used to determine peak concentration). This value was 26.6  $\pm$  1.4 nM (mean  $\pm$  SE). Clomipramine was adsorptive and was not usually detected at concentrations <100  $\mu$ M in vitro. Figure 1, C and D shows a postexperimental calibration trial for 5-HT and clomipramine, respectively.

### Drug administration and positioning of electrodes

Serotonin (Sigma, St. Louis, MO) was administered to the spinal cord by intraspinal microinjection or dorsal surface application (superfusion). In some 5-HT microinjection trials, clomipramine (RBI, Natick, MA) was microinjected into the cord. Experimental sessions typically consisted of several separate trials of 5-HT administration only (spaced by tens of minutes), followed by trials with clomipramine and 5-HT. Drugs were dissolved in PBS (pH = 7.4) or aCSF (pH = 7.3).

For microinjection experiments, a yoked array of two to three CFMEs and drug/vehicle ejection electrodes (pulled glass micropipette with a 25- to 50- $\mu$ m-diameter tip) were typically mounted on independently controlled microdrives of a double manipulator (Bras et al. 1990). The drug electrode and nearest CFME (viewed through a Peak Stand Microscope,  $\times$ 100) were positioned in the same medial-lateral plane and at a fixed distance from each other in the rostrocaudal plane with an X-Y micropositioner (which held the drug electrode to the microdrive). The

double manipulator allowed the independent lowering of the drug pipette(s) into the spinal cord to the same depth (Z axis) as the CFMEs (cf. Zahniser et al. 1998), which were then positioned into either the dorsal horn, intermediate zone, or ventral horn of spinal segments L1–S2. A trial consisted of ejecting the drug at a constant rate of 0.1–4.0  $\mu\text{l}/\text{min}$ , to deliver a volume of 0.5–3.5  $\mu\text{l}$  of solution. Flow was controlled by a CMA 102 microdialysis syringe pump. Thus microinjection experiments provided data on the rostral–caudal spread of 5-HT in the spinal cord.

During superfusion trials, the bathing medium was rapidly removed by suction. Serotonin was then quickly and uniformly applied (at 37°C) to the dorsal surface of the spinal cord, remaining there undisturbed until washout. Typically, a trial was followed with restoration of the bathing medium by rapid suction and repeated washout. In these superfusion experiments, the two to four CFMEs were lowered to various locations within the L1–S2 spinal cord (in the dorsal horn, intermediate zone, or ventral horn) sometimes in adjacent, spinal segments, but always maintaining a similar medial–lateral (within 100  $\mu\text{m}$ ) and rostral–caudal (1.5–4 mm) position within each experimental trial. In one experiment, the yoked array of CFMEs was moved between trials to a new vertical position. Thus superfusion experiments provided data on the dorsoventral concentrations of 5-HT obtained after surface application to the spinal cord.

### Data analysis

Measurements made for each CFME included: oxidation onset latency (OxOnset), time-to-peak of the oxidation current (TTP), percentage of initial concentration applied to the cord, and time for 50 and 100% decay (to baseline) of the 5-HT oxidation signal ( $D_{50}$  and  $D_{100}$ , respectively). All values were measured from time of 5-HT application. If an electrode was repositioned during a trial only concentration data were collected. To examine the effect of clomipramine on the spread of 5-HT, the responses to application of 5-HT immediately before and after clomipramine administration were compared. Group means were compared by ANOVA. The relationship between response measures and spatial parameters was examined using Pearson product-moment correlation. In some cases, the presence or absence of a response was compared using nonparametric chi-square test of independence. Post hoc tests used Fisher's PLSD (protected least-significant difference). A level of  $P < 0.05$  was considered significant.

### Histology and determination of electrode position

At the end of the experiment the spinal cord was removed and immersed in 4% paraformaldehyde, embedded in paraffin, then serially sectioned (10–14  $\mu\text{m}$  thickness) and stained with cresyl violet. Drawings were made to reconstruct the position of the electrode tracks. Electrode tip positions (lamina and laterality) were determined from micromanipulator depth measurements (calculated from insertion point on dorsal surface of spinal cord) along electrode track reconstructions, after allowing for a slight degree of tissue shrinkage (~5%). For microinjection experiments, the distance between the CFMEs and microinjection site was preset as described previously. For superfusion experiments, the depth of the microelectrode was defined as the shortest distance from the CFME tip position to the spinal cord surface exposed by the laminectomy. The spinal segment was determined at the time of dissection by examination of the exit of ventral–dorsal roots.

## RESULTS

### In vivo confirmation of voltammetric signals

The oxidation peaks for 5-HT were slightly delayed in vivo (Fig. 2) compared with in vitro (Fig. 1) (Hentall et al. 2006; Noga et al. 2004; Phillips and Stamford 1999) and oftentimes the oxidation current developed a shoulder during the course of the experiment, as described



previously (Phillips and Stamford 1999). The reduction peaks also tended to be broader and were slightly displaced (cf. Figs. 1 and 2). Reduction peaks were typically smaller than oxidation peaks and, at low concentrations or as concentrations decreased, one or both of the reduction signals could become indistinguishable from baseline noise levels (Stamford et al. 1992). Thus in color plots the reduction peaks would sometimes “disappear” (Fig. 2), despite the fact that oxidation currents were still visible. Nevertheless in this circumstance, the evolving signals were interpreted as being due to 5-HT.

### Microinjection of 5-HT

The goal of microinjecting 5-HT into the spinal cord was to determine the temporal and spatial spread of 5-HT, from the focal injection site to proximal areas of the cord. Spread of 5-HT within the gray matter was examined in the rostrocaudal plane, and assumed to be equal in all directions (Prokopová et al. 1997). In these experiments (seven animals), the tips of the CFMEs were spaced 400–2,800  $\mu\text{m}$  from the tip of the drug micropipette, at the same depth and lamina in the lumbosacral spinal cord. All of the microinjection experiments were performed medial to the dorsal root entry zone within laminae III–VII and using 100  $\mu\text{M}$  5-HT. Usually, three to six trials were performed with the same CFMEs. A typical example of the spread of 5-HT within the spinal cord after its microinjection as detected by individual CFMEs located at different distances away from the microinjection site is illustrated in Fig. 2. Note the diminishing response and the increased TTP of the 5-HT oxidation current with increasing distance from the site of microinjection.

To analyze the dependence of distance on the detection of 5-HT (response vs. nonresponse) from a point source, CFMEs were grouped into three rostrocaudal categories (Fig. 3A): 1) *Close*: <1 mm away (400–800  $\mu\text{m}$ ;  $n = 33$ ); 2) *Intermediate*: between 1 and 2 mm away (1,150–1,950  $\mu\text{m}$ ;  $n = 17$ ); 3) *Far*:  $\geq 2$  mm away from the drug micropipette (2,000–2,800  $\mu\text{m}$ ;  $n = 16$ ). A 2 (current detected vs. no current detected)  $\times$  3 (position groups) chi-square test compared the occurrence of 5-HT oxidation currents, and revealed significant variation among position groups in whether they detected 5-HT [ $\chi^2(2, n = 66) = 21.7, P < 0.0001$ ]. As shown in Fig. 3A, there was a negative relationship between increasing electrode distance and detection of 5-HT. Preliminary analysis and theoretical expectations suggested that smaller responses would occur at more distant locations, so we placed the most sensitive CFMEs (as determined by preexperimental calibration) there. Even with this bias, it is apparent that an insignificant fraction of 5-HT (microinjected in volumes  $\leq 3.5 \mu\text{l}$ ) travels beyond a 2-mm radius in the rostrocaudal axis of the lumbosacral spinal cord.

There was a significant negative relationship between the percentage of initial concentration and distance of the CFME from the site of microinjection [100  $\mu\text{M}$  5-HT; Pearson product-moment correlation =  $-0.43$  ( $r^2 = 0.19$ ),  $F(1,65) = 14.58, P = 0.003$ ]. Concentrations of 5-HT at different distances from the site of microinjection are plotted in Fig. 3B. As seen in this plot, as distance increased 5-HT concentrations decreased dramatically. On average, electrodes within 1 mm of the site of injection (*Close*) detected 1.43  $\mu\text{M}$  5-HT, corresponding to 1.43% of the initial concentration, whereas CFMEs in the *Intermediate* and *Far* positions detected 0.28 and 0.03  $\mu\text{M}$ , respectively. These were significantly different [one-way ANOVA:  $F(2,63) = 7.35, P = 0.001$ ]. Thus within just 1 mm from the site of injection, the concentration of microinjected 5-HT within the extracellular space had already decreased by >98%.

Diffusion parameters of 5-HT through the spinal cord after microinjection were also explored (Fig. 4). Pearson product-moment correlations showed significant positive associations between OxOnset and CFME distance [0.4;  $r^2 = 0.16, F(1,43) = 7.88, P = 0.008$ ] and between TTP and CFME distance [0.46;  $r^2 = 0.19, F(1,43) = 11.33, P = 0.002$ ]. The average OxOnset for electrodes within 1 mm of the injection site was  $67.1 \pm 6.3$  s, compared with electrodes at greater distances ( $598.2 \pm 170.7$  s). Earlier OxOnsets were associated with a quicker TTP

(not shown), whereas later OxOnsets were associated with longer TTPs [ $0.95; r^2 = 0.91; F(1,43) = 401.28, P = 0.001$ ]. 5-HT microinjections administered at the lowest volume ( $0.25 \mu\text{l}$ ) and rate ( $\leq 0.25 \mu\text{l}/\text{min}$ ) resulted in higher mean values for OxOnset and TTP. For example, OxOnset was about 2.5-fold faster with a microinjection rate of  $0.50$  (OxOnset =  $50$  s) compared with  $0.25 \mu\text{l}/\text{min}$  (OxOnset =  $120$  s). Any decreases in the OxOnset latencies seen with greater distances were associated with the use of more sensitive electrodes at the more distant locations (tending to bias the values toward earlier detection).

Overall, the relationship of CFME distance with  $D_{50}$  or  $D_{100}$  was not significant by the Pearson product-moment correlation (see Fig. 4A for  $D_{50}$ ), although CFMEs in the *Close* positions took significantly less time to decay to 50% ( $D_{50}$ ) compared with CFMEs in *Intermediate* positions [ $F(2,39) = 5.98, P = 0.005$ ]. These results indicate that at close proximity to a site of microinjection, decay times of 5-HT (as well as OxOnset and TTP; see previous paragraph) were strongly affected by the movement/diffusion of a bolus of 5-HT through the tissue, rather than reuptake mechanisms only.

Higher concentrations also required longer times to decline completely to baseline, as indicated by a positive relationship [ $0.64; r^2 = 0.40; F(1,26) = 16.94, P < 0.001$ ] observed between concentration and  $D_{100}$  (Fig. 4B). Interestingly, no relationship was observed for  $D_{50}$ . This further suggests that after microinjection, there may be at least two different mechanisms for removal of 5-HT, one that is concentration dependent and one that is not.

Control vehicle injections ( $n = 6$ ) were performed to verify that CFME responses observed after microinjection were due to 5-HT, and not to other physical or chemical factors (e.g., a pressure wave, ionic differences, etc.) that may be associated with microinjection per se. Control vehicle injections did not produce 5-HT electrochemical signals, although any slight changes in baseline signal were most pronounced on electrodes nearest the site of injection.

### Superfusion of 5-HT

The spinal cord was superfused with 5-HT to determine its temporal and spatial spread from the convex dorsal surface to deeper sections of the lumbosacral cord. This was a near-instantaneous and uniform application of 5-HT across the dorsal surface of the spinal cord that essentially provided a continuous source of the neurotransmitter (until washout of the bath solution). In these experiments (seven animals), the tips of two to four CFMEs were lowered into the dorsal horn, intermediate zone, and ventral horn. 5-HT was administered at various concentrations ( $5, 10, 100, \text{ or } 1,000 \mu\text{M}$ ). Washout of the bath solution was done at various times after 5-HT application and the spinal cord bathed in control vehicle solution between trials, as described in METHODS.

Following superfusion of 5-HT, two responses could be observed (Fig. 5). In most cases ( $16/18$ ), 5-HT signals were rapidly elevated (within  $30$  s). This initial response was often transient and oxidation signals returned to baseline or near-baseline levels within minutes of application. This type of response is illustrated in Fig. 5A (see also Fig. 5C) for a  $100 \mu\text{M}$  5-HT superfusion trial. In this example, 5-HT levels peaked within  $4 - 12$  s of application, with concentrations being largest in the dorsal horn ( $0.13 \mu\text{M}$  or  $0.13\%$  of the applied concentration). Prolonged exposures sometimes also revealed a second increase in oxidation current (Fig. 5B and C), which lasted until washout. These sustained responses were found with superfusions of  $\geq 100 \mu\text{M}$  (Fig. 6A).

To analyze the dependence of depth (to closest surface area exposed by the laminectomy) on the detection of bath-applied 5-HT (response vs. nonresponse), CFMEs were grouped into three categories: 1) *Superficial*:  $\leq 400 \mu\text{m}$  from surface; 2) *Middle*: between  $401$  and  $800 \mu\text{m}$ ; and 3) *Deep*:  $\geq 801 \mu\text{m}$ . Histological analysis showed *Superficial* CFMEs within laminae I and II

(100–400  $\mu\text{m}$  deep), *Middle* CFMEs within laminae II–IV (470–600  $\mu\text{m}$  deep), and *Deep* CFMEs within laminae V, VII, and VIII, and ventral white matter (850–1,600  $\mu\text{m}$  deep). An overall 2 (current detected vs. no current detected)  $\times$  3 (position groups) chi-square test did not detect any significant difference among the groups [ $\chi^2(2, n = 40) = 4.95, P = 0.08$ ]. However, because we hypothesized that superficially positioned electrodes would show a greater likelihood of response than deeper electrodes, we compared separately the incidence of 5-HT oxidation currents between each group using a 2 (current detected vs. no current detected)  $\times$  2 (position groups) chi-square test. With this analysis a significant difference was detected, with electrodes in *Superficial* positions detecting 5-HT more often than *Middle* [ $\chi^2(1, n = 29) = 4.97, P = 0.03$ ] or *Deep* electrodes [ $\chi^2(1, n = 19) = 3.69, P = 0.05$ ]. All 8/8 CFMEs in *Superficial* positions detected 5-HT, whereas 12/21 (57%) and 7/11 (64%) of CFMEs in *Middle* and *Deep* positions detected 5-HT, respectively.

The maximum concentrations of 5-HT detected at various depths from the exposed dorsal surface of the spinal cord after bath application of 5-HT (5–1,000  $\mu\text{M}$ ) are plotted in Fig. 6A. Two features stand out with this analysis. First, a relatively small amount of 5-HT was detected even at the most superficial depths sampled, indicating that the dorsal surface of the spinal cord poses a significant barrier to the penetration of 5-HT. Second, the concentrations were rapidly attenuated with increasing depth. These features are illustrated best from trials in which 1,000  $\mu\text{M}$  of 5-HT was applied. A Pearson product-moment correlation assessing the relationship between the percentage of initial concentration and CFME depth was  $-0.58 (r^2 = 0.33)$ , which was significant [ $F(1,19) = 9.02, P = 0.008$ ]. A one-way ANOVA also indicated a significant difference among position groups in the percentage of initial concentration detected [ $F(2,17) = 4.33, P = 0.03$ ], confirming this correlation. On average (mean  $\pm$  SE), with superfusion of 1,000  $\mu\text{M}$  5-HT, electrodes at *Superficial* positions detected 2.5  $\mu\text{M}$  5-HT ( $0.25 \pm 0.12\%$ ;  $n = 6$ ), whereas *Middle* and *Deep* CFMEs detected 0.49 and 0.01  $\mu\text{M}$  5-HT ( $0.05 \pm 0.02\%$ ;  $n = 8$ ; and  $0.001 \pm 0.01\%$ ;  $n = 6$ ), respectively.

The amount of 5-HT crossing the arachnoid and pia membranes and entering the spinal cord after superfusion was significantly less than that observed with diffusion of 5-HT through spinal gray matter after intraspinal microinjection (cf. Figs. 3B and 6A). This was evident when the extracellular concentration of 5-HT given at 100  $\mu\text{M}$  was compared for electrodes at similar distances (between 470 and 600  $\mu\text{m}$ ) from the site of application in both protocols:  $2.44 \pm 0.7 \mu\text{M}$  or 2.44% for microinjection and  $0.33 \pm 0.16 \mu\text{M}$  or 0.33% for superfusion [ANOVA test:  $F(1,19) = 13.28, P = 0.002$ ]. This implies that other factors, in addition to diffusion, substantially impede the movement of 5-HT into the spinal cord when it is administered from the dorsal surface. Compared with bath application, microinjection can therefore deliver higher drug concentrations to restricted areas of the spinal cord.

Parameters of 5-HT diffusion through the spinal cord after superfusion were also examined (Fig. 6, B–D). In the trials using 100  $\mu\text{M}$  5-HT, there was no significant relationship between electrode depth and OxOnset, TTP,  $D_{50}$ , or  $D_{100}$  latencies. Using ANOVA tests to compare response times between superfusion and microinjection trials for electrodes at similar distances (470 – 600  $\mu\text{m}$  away) from the site of 100  $\mu\text{M}$  5-HT application, OxOnset was significantly faster after superfusion ( $13.2 \pm 7.0$  s) than microinjection ( $51.4 \pm 5.1$  s) [ $F(1,5) = 20.59, P = 0.006$ ]. Both  $D_{50}$  and  $D_{100}$  clearance times were also significantly faster after superfusion than microinjection in this comparison [for  $D_{50}$ :  $F(1,5) = 35.64, P = 0.002$ ; for  $D_{100}$ :  $F(1,5) = 26.04, P = 0.004$ ]. Superfusion and microinjection  $D_{50}$  values were  $132.0 \pm 66.6$  and  $523.9 \pm 29.3$  s, respectively. Superfusion and microinjection  $D_{100}$  values were  $161.7 \pm 82.4$  and  $1,323 \pm 183.3$  s, respectively. This is to be expected for overall lower concentrations observed in superfusion trials, considering that high 5-HT concentrations take longer than low concentrations to decline completely to baseline (see Fig. 4B).



## Effect of clomipramine on the spread of 5-HT

Clomipramine was used to evaluate the effect of blocking SERT on the spatiotemporal spread of 5-HT. Clomipramine was used in microinjection experiments because microinjection of 5-HT produced a stronger and more robust effect than superfusion of 5-HT. In previous studies in brain tissue, transporter blockers have been shown to prolong the presence of neurotransmitter in the extracellular space (Bunin and Wightman 1998; Daws et al. 1997, 2005) and only occasionally increase the amplitude of the signal, thus increasing the concentration of detected neurotransmitter (Daws et al. 2005; Montañez et al. 2003; Zahniser et al. 1998). Therefore we compared the  $D_{50}$  and  $D_{100}$  latencies and the percentage of initial concentration for a 5-HT microinjection made before administration of clomipramine (PreClom) and after administration of clomipramine (PostClom). PostClom responses were expressed as a percentage of the PreClom response.

When clomipramine was microinjected into the spinal cord, the clomipramine micropipette was positioned either adjacent to the 5-HT micropipette or separated from the 5-HT micropipette by at least one CFME. After an initial 5-HT microinjection(s) (100  $\mu$ M), clomipramine (10–100  $\mu$ M) was microinjected, and then 5-HT was microinjected again. Up to two PostClom 5-HT microinjections were administered, the latest being  $\leq 1,550$  s from the time of clomipramine administration. The clomipramine trials commenced after baseline data on the spread of microinjected 5-HT (see *Microinjection of 5-HT*) was obtained ( $n = 7$  animals).

There was no overall statistically significant difference between the 5-HT microinjection for the percentage of initial concentration,  $D_{50}$ , or  $D_{100}$  latencies, before and after clomipramine. However, the PostClom responses were slightly higher/longer than the PreClom responses (see Fig. 7A):  $122.8 \pm 19.9\%$  of PreClom concentration;  $115.2 \pm 17.2\%$  of PreClom  $D_{50}$ ;  $133.3 \pm 59.0\%$  of PreClom  $D_{100}$ . This is in keeping with the relatively small effects of SERT inhibition observed in other studies (Bunin and Wightman 1998; Daws et al. 2000). Additionally, treatment with clomipramine provoked responses to 5-HT microinjection in two of nine CFMEs located distally ( $\sim 2$  mm away from the site of microinjection) that previously showed no response. These CFMEs detected 0.26 and 0.65  $\mu$ M 5-HT, which are well above the mean detected in PreClom trials of responsive *Far*-positioned CFMEs (0.03  $\mu$ M; see previous text). In one of the seven experiments, we also observed in two separate trials a decremting response at two CFMEs to repeated microinjection of 5-HT when given in close succession to each other (microinjections within 18 min of each other). This was reversed in both cases after microinjection of clomipramine (Fig. 7B) but only one trial is shown. These observations all support the suggestion that clomipramine affected reuptake by the SERT and promoted the spread of 5-HT within the cord.

## DISCUSSION

Serotonin has been shown to facilitate/modulate locomotor rhythms (e.g., Barbeau and Rossignol 1991; Cazalets et al. 1992; Cowley and Schmidt 1994; Feraboli-Lohnherr et al. 1999), nociception or antinociception (e.g., Bardin et al. 1997; Lopez-Garcia 1998; Schmauss et al. 1983; Xu et al. 1994), sympathetic nerve activity/thermogenesis (Madden and Morrison 2006), and spinal plasticity (e.g., Crown and Grau 2005) using microinjection, intrathecal, and/or bath-application methods. The present study provides the first systematic examination of the spatiotemporal spread of exogenously applied 5-HT in the spinal cord in real time. Using FCV to measure extracellular 5-HT at CFMEs after intraspinal microinjection or bath application (superfusion of the dorsal surface), we show that different methods of delivery can yield different and varying levels of 5-HT within the spinal cord at a given location and time.

### Dorsal surface application and intraspinal microinjection of 5-HT

For superfusion of 5-HT, concentration gradients within the spinal cord are steep, so that only a relatively low percentage of the applied 5-HT is achieved within the cord. Baseline extracellular concentrations of 5-HT are typically quite rapidly restored after the initial response to 5-HT application, implying a strong homeostasis of endogenously released 5-HT in the spinal cord. Superfusion leads to relatively small amounts of 5-HT entering the spinal cord gray matter, with <0.8% of the bath solution concentration being detected in the superficial dorsal horn (within 400  $\mu\text{m}$  of the surface). Even smaller amounts of 5-HT reach the intermediate zone and ventral horn.

The concentration of 5-HT is also rapidly attenuated when it is microinjected into the spinal cord. However, nearly tenfold the 5-HT concentration is measured after microinjection compared with bath superfusion at equivalent distances from the site of 5-HT application. This disparity is likely due to the presence of additional diffusion barriers that the superfused 5-HT must cross before entering the spinal cord. With our microinjection protocol, the 5-HT must travel only through gray matter from the drug micropipette to reach the CFMEs, which are all positioned at the same depth in the cord and thus in the same horizontal plane and lamina. Therefore diffusion to the CFME from the microinjection pipette may be assumed to be relatively uniform (Rice et al. 1993). With superfusion, the 5-HT must first penetrate the surface arachnoid and pia (except at the location of insertion of CFMEs; see METHODS) and then diffuse through various compartments of white and/or gray matter, which significantly differ in their diffusion properties (Syková 2004). These are likely the most important factors limiting the amount of 5-HT entering the cord after superfusion. Once in the spinal cord, other factors such as the efficacy of clearance mechanisms, the tissue volume fraction, and the tortuosity (Nicholson and Syková 1998; Syková et al. 2000) become important. Parameters such as tortuosity and volume fraction are only slightly different in the dorsal horn, intermediate zone, and ventral horn of the rat lumbar spinal cord (Šimonová et al. 1996; Syková et al. 1994). Furthermore, the density of SERT is only slightly nonuniform and correlated with the serotonergic innervation pattern of the spinal gray matter (Sur et al. 1996). Therefore these factors should be affecting 5-HT diffusion within the spinal cord similarly in both protocols.

The 5-HT oxidation onset and TTP values were significantly shorter for CFMEs positioned closest to the area of 5-HT microinjection. However, there was no significant relationship between electrode depth and OxOnset and TTP in superfusion trials. In addition, the OxOnset was significantly faster after superfusion than that after microinjection, occurring within 30 s of application at all depths (compared with >30 s for nearly all responses in the microinjection trials at any depth). These differences may be explained by the fact that with superfusion, 5-HT is applied instantaneously to a large convex surface, whereas with microinjection 5-HT is applied relatively slowly (>1 min or so) to one point. Alternatively, or in addition, small openings in the arachnoid and pia may have allowed a small quantity of 5-HT within the bath to transiently flow down the side of the CFMEs, thus bypassing potential diffusion barriers. Even so, this latter possibility is likely only minor considering the significant discrepancy between the concentrations attained between bath application and microinjection discussed in the previous paragraph.

The working hypothesis of this study predicted that applied serotonin would not travel far from its source. This is borne out both with pulsed (microinjection) and with prolonged (superfusion) application, in that concentrations were essentially undetectable beyond 1 mm or so, for a wide range of applied doses. However, local confinement may not readily account for the second, gradual increase in oxidation current within the spinal cord after prolonged bath application of 5-HT (Figs. 5, B and C and 6A). Sustained responses were sometimes found with superfusion of  $\geq 100 \mu\text{M}$  and peaked within 10 min of application. Although it is possible that this increase in oxidation signal could be related to the detection of 5-HT metabolites (see Noga et al.

2004), longer-latency responses to intrathecal application of 5-HT in the adult rat have been described. Feraboli-Lohnherr et al. (1999) noted stabilization of interlimb coordination during rhythmic motor activity induced in spinal rats within 5 min of application of 5 mM 5-HT. Maximal effects of 5-HT on the duration of this rhythmic activity occurred by 10 min. Furthermore, Glaum et al. (1990) reported that 5-HT increased nociceptive thresholds within 5 min. In preparations using smaller spinal cords and lower concentrations, quicker responses to bath superfusion of 5-HT have been observed. Cowley and Schmidt (1994) reported an “immediate increase” in tonic and slower induction (1–3 min) of rhythmic hindlimb nerve activity with bath application of 10–100  $\mu$ M 5-HT to the isolated neonatal rat spinal cord. In a similar preparation, Kiehn and Kjærulff (1996) described induction of rhythmic activity with 10–100  $\mu$ M 5-HT within 30–90 s of application. These quick responses may be mediated by an equivalent process to the early diffusion response observed in the present study.

### Effect of clomipramine on the spread of microinjected 5-HT in the spinal cord

To examine the effect of SERT on clearance, we measured the spatiotemporal spread of exogenously applied 5-HT after application of the SERT inhibitor clomipramine. It has been shown that 5-HT clearance in the dorsal raphe nucleus is prolonged but that concentrations remain unchanged during blockade of SERT and 5-HT receptors (Bunin and Wightman 1998). Likewise, SERT blockade prolongs the extracellular clearance of locally applied exogenous 5-HT in the dentate gyrus of the hippocampus (Daws et al. 1997). Clomipramine also has been shown to significantly influence SERT activity in the hypothalamus (Marinesco et al. 1996). Based on this previous work in the brain, we expected that clomipramine would prolong the presence/clearance of 5-HT in the extracellular space. Although we found no overall significant effect of clomipramine on the spread of 5-HT, results were in the predicted direction and an effect of clomipramine was apparent in many cases (e.g., Fig. 7).

The reason for the overall lack of significance of an effect of SERT blockade in the spinal cord in the present study is not clear, although several possibilities may help explain this difference from studies in other neural regions. It has been shown that clearance of 5-HT is reduced when SERT function is inhibited by >90% (Montañez et al. 2003). However, when as few as 20% of SERT is spared, normal clearance of 5-HT occurs. It is possible that clomipramine concentrations in the present study were insufficient to fully block SERT uptake of 5-HT. Another possibility is that there is a difference in the density of different types of transporters between the brain and spinal cord, with perhaps more clearance by heterogeneous transporters in the cord. In addition to SERT, 5-HT uptake can occur by the dopamine transporter (DAT; Jackson and Wightman 1995; Zhou et al. 2002) and the norepinephrine transporter (NET; Daws et al. 1998, 2005), with uptake rates and binding affinity varying according to brain region (Daws et al. 2005). Thus blocking SERT function may have led to an upregulation of DAT and NET activity in the spinal cord for removal of 5-HT, as suggested by the model of cooperative binding interactions by Daws and colleagues (2005). It is also possible that SERT blockade has less of a dampening effect on the spread of 5-HT when the concentration of 5-HT is high than when it is at a more physiological level. In summary, the findings that baseline extracellular 5-HT concentrations are rapidly restored, do not increase drastically after experimental application, and that treatment with a SERT inhibitor does not significantly influence exogenously applied 5-HT suggest that several other compensatory and redundant homeostatic mechanisms exist in the spinal cord to maintain 5-HT levels. Given the type of preparation used here, we cannot exclude the possibility that some of these mechanisms are mediated by descending brain pathways or presynaptic mechanisms instead of only local spinal circuitry or postsynaptic effects.

## Implication of the findings

The findings of this study may also be applicable to other preparations that utilize spinal microinjection and bath-application methodologies. For example, one of the most commonly used preparations to study the neural mechanisms of locomotion is the *in vitro* neonatal rat spinal cord, which may include attached brain stem, nerves, and/or hindlimbs (for review see Clarac et al. 2004). Once placed in a superfusion/recording chamber, neuroactive substances can be added to the bathing solution to examine their effects on spinal function. Typically, spinal cords are much smaller (with higher surface area/volume ratios) and drugs are applied to all surface areas. We therefore can expect that concentration profiles will be somewhat higher in this preparation for the same concentration of bath-applied 5-HT compared with our study in the adult spinal cord with dorsal surface application. The degree of this difference remains to be determined. However, with respect to distance from surface (site of application) as measured in the present study, we would expect a maximum of about 0.06–1% of the applied concentration of 5-HT (see Fig. 6) at a distance of about 500  $\mu\text{m}$  from surface. This would translate to about 60–1,000 nM, of an applied 100  $\mu\text{M}$  5-HT at the core of the neonatal rat spinal cord (assuming a width of  $\sim 1$  mm for the neonatal rat cord; Kjærulff and Kiehn 1996). These concentrations would be sufficient to activate 5-HT<sub>1A,1B,2C,4,6,7</sub> but not 5-HT<sub>2A</sub> receptors (see Table 3.3 of Hochman et al. 2001).

Other developmental factors will also affect the diffusion of neurotransmitters into neonatal rat spinal cord. Changes in extracellular space diffusion parameters occur over the first couple of postnatal weeks, including a decrease in the extracellular space volume fraction, an increase in tortuosity, and an increase in anisotropy with the appearance of myelin (Prokopová et al. 1997; Syková and Chvátal 1993). Last, developmental changes occur in the pia–arachnoidal membranes over the first three postnatal weeks, resulting in an increase in the amount of extracellular collagenous and elastic fibers (McLone and Bondareff 1975). This thickening of the membranes may be somewhat counteracted by the appearance of fenestrations in the adult rat pia (Morse and Low 1972), which may facilitate 5-HT entrance into the spinal cord. Fenestrations are also observed in human lumbar pia mater (Reina et al. 2004).

It is unknown whether other neurotransmitters penetrate the pia more readily than 5-HT or show the same pattern of spatiotemporal spread in the spinal cord after bath application or microinjection. Characterization of the spatiotemporal spread of an applied neurotransmitter within a trial requires sampling at more than one site, as was done in this study. Several previous studies have obtained measurements of neurotransmitter concentrations and clearance in the CNS at a single location, using a single recording electrode positioned at a fixed distance from the site of microinjection (e.g., Daws et al. 1997, 2005; Zahniser et al. 1998). Binns et al. (2005) simultaneously recorded from up to four intraspinal sites after microinjection of glutamate into the spinal cord. However, the latency for detection of the microinjected neurotransmitter at the different sites was not a focus of their study. Therefore the results obtained in the present study cannot be directly compared with those obtained in the preceding studies using microinjection. We are not aware of any studies that have looked at the intraspinal diffusion of neurotransmitters after bath application. Thus the penetration of neurotransmitters other than 5-HT through the pia remains to be determined. It is interesting to note, however, that preliminary evidence from our laboratory in the adult cat suggests that other monoamines (e.g., norepinephrine) show a similar dorsal–ventral spread after dorsal surface application (Brumley et al. 2007). It will be important to perform further studies to confirm these findings.

The spatiotemporal pattern of endogenously released 5-HT observed within the lumbar spinal cord after electrical stimulation of the raphe nuclei (Hentall et al. 2006) differs somewhat from that seen with exogenously applied 5-HT. A moderately uniform release of 5-HT is seen in gray matter during raphe stimulation, with peak extracellular concentrations averaging approximately 38 nM (maximum 287 nM). Higher concentrations were found in the dorsal and

ventral horn than in the intermediate zone. Based on our results with superfusion of 5-HT to the dorsal surface of the rat spinal cord, one could predict that a similarly polarized but steeper concentration gradient (lower concentrations within the core areas of the cord) would be observed after intrathecal injection of 5-HT (assuming uniform distribution in the intrathecal space). In contrast, intraspinal microinjection could be used to achieve higher concentrations of 5-HT in focal areas of the cord, including those in deeper regions.

In conclusion, this study shows that after spinal application of 5-HT, the 5-HT concentrations attained in the mammalian spinal cord, where locomotor and pain circuitry is present (e.g., Cina and Hochman 2000; Dai et al. 2005; Willis and Westlund 1997), will depend on the method used. Factors to consider are the concentrations used, the distance between site of application and target area containing the receptors of interest, the presence (or absence) of physical barriers, and the location and density of transporters relative to the site of application and the target area. Caution should be exercised when interpreting changes in spinal activity after manipulations that change diffusion distances and clearance parameters. For example, spinal lesions performed in a bath environment not only will sever certain pathways but also will effectively increase local drug concentration and subsequently the degree and type of ligand–receptor interaction.

## Acknowledgements

We thank B. Ballester, D. Ospina, and D. Pabon-Ramon for assistance during some of the experiments.

### GRANTS

This study was supported by National Institute of Neurological Disorders and Stroke Grant NS-46404, The Miami Project to Cure Paralysis, and by a grant from the State of Florida.

## References

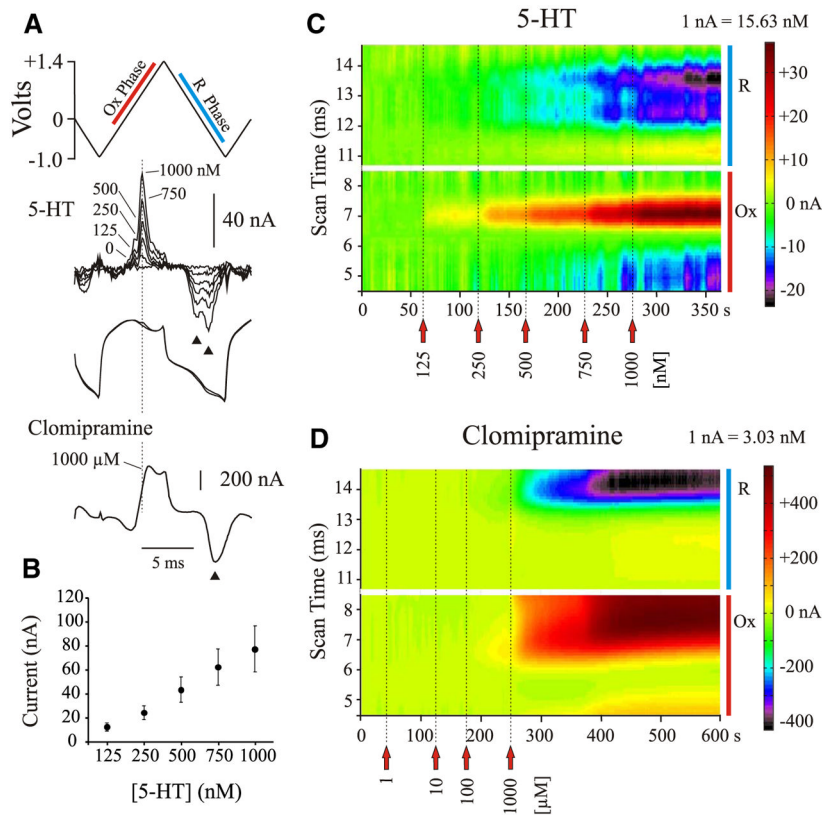
- Antri M, Orsal D, Barthe J-Y. Locomotor recovery in the chronic spinal rat: effects of long-term treatment with a 5-HT<sub>2</sub> agonist. *Eur J Neurosci* 2002;16:467–476. [PubMed: 12193190]
- Armstrong-James, M.; Millar, J. High-speed cyclic voltammetry and unit recording with carbon fibre microelectrodes. In: Marsden, CA., editor. *Measurement of Neurotransmitter Release In Vivo*. Toronto: Wiley; 1984. p. 209-226.
- Barbeau H, Rossignol S. Initiation and modulation of the locomotor pattern in the adult chronic spinal cat by noradrenergic, serotonergic, and dopaminergic drugs. *Brain Res* 1991;546:250–260. [PubMed: 2070262]
- Bardin L, Bardin M, Lavarenne J, Eschalier A. Effect of intrathecal serotonin on nociception in rats: influence of the pain test used. *Exp Brain Res* 1997;113:81–87. [PubMed: 9028777]
- Binns BC, Huang Y, Goettl VM, Hackshaw KV, Stephens RL. Glutamate uptake is attenuated in spinal deep dorsal and ventral horn in the rat spinal nerve ligation model. *Brain Res* 2005;1041:38–47. [PubMed: 15804498]
- Brumley MR, Taberner AM, Blythe AD, Sanchez FJ, Hentall ID, Noga BR. Serotonin and norepinephrine concentrations measured simultaneously at various depths in the lumbar spinal cord of the adult cat following dorsal surface (bath) application. *Soc Neurosci Abstr* 2007;33:924.15.
- Bunin MA, Wightman RM. Quantitative evaluation of 5-hydroxytryptamine (serotonin) neuronal release and uptake: an investigation of extrasynaptic transmission. *J Neurosci* 1998;18:4854–4860. [PubMed: 9634551]
- Cazalets JR, Sqalli-Houssaini Y, Clarac F. Activation of the central pattern generators for locomotion by serotonin and excitatory amino acids in neonatal rat. *J Physiol* 1992;455:187–204. [PubMed: 1362441]
- Cina C, Hochman S. Diffuse distribution of sulforhodamine-labeled neurons during serotonin-evoked locomotion in the neonatal rat thoracolumbar spinal cord. *J Comp Neurol* 2000;422:590–602. [PubMed: 10880990]



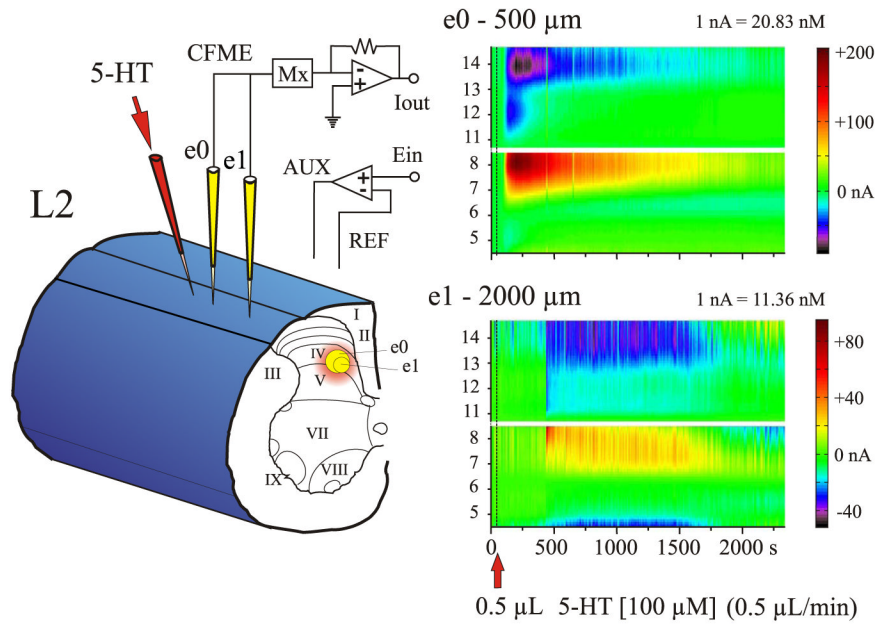
- Clarac F, Pearlstein E, Pflieger J-F, Vinay L. The in vitro rat spinal cord preparation: a new insight into mammalian locomotor mechanisms. *J Comp Physiol A Sens Neural Behav Physiol* 2004;190:343–357.
- Cowley KC, Schmidt BJ. A comparison of motor patterns induced by *N*-methyl-D-aspartate, acetylcholine and serotonin in the in vitro neonatal rat spinal cord. *Neurosci Lett* 1994;171:147–150. [PubMed: 8084477]
- Crown ED, Grau JW. Evidence that descending serotonergic systems protect spinal cord plasticity against the disruptive effect of uncontrollable stimulation. *Exp Neurol* 2005;196:164–176. [PubMed: 16139268]
- Dai X, Noga BR, Douglas JR, Jordan LM. Localization of spinal neurons activated during locomotion using the c-fos immunohistochemical method. *J Neurophysiol* 2005;93:3442–3452. [PubMed: 15634712]
- Daws LC, Gould GG, Teicher SD, Gerhardt GA, Frazer A. 5-HT<sub>1B</sub> receptor-mediated regulation of serotonin clearance in rat hippocampus in vivo. *J Neurochem* 2000;75:2113–2122. [PubMed: 11032901]
- Daws LC, Montañez S, Owens WA, Gould GG, Frazer A, Toney GM, Gerhardt GA. Transport mechanisms governing serotonin clearance in vivo revealed by high-speed chronoamperometry. *J Neurosci Methods* 2005;143:49–62. [PubMed: 15763136]
- Daws LC, Toney GM, Davis DJ, Gerhardt GA, Frazer A. In vivo chronoamperometric measurements of the clearance of exogenously applied serotonin in the rat dentate gyrus. *J Neurosci Methods* 1997;78:139–150. [PubMed: 9497010]
- Daws LC, Toney GM, Gerhardt GA, Frazer A. In vivo chronoamperometric measures of extracellular serotonin clearance in rat dorsal hippocampus: contribution of serotonin and norepineprine transporters. *J Pharmacol Exp Ther* 1998;286:967–976. [PubMed: 9694957]
- Feraboli-Lohnherr D, Barthe J-V, Orsal D. Serotonin-induced activation of the network for locomotion in adult spinal rats. *J Neurosci Res* 1999;55:87–98. [PubMed: 9890437]
- Fong AJ, Cai LL, Ootoshi CK, Reinkensmeyer DJ, Burdick JW, Roy RR, Edgerton VR. Spinal cord-transected mice learn to step in response to quipazine treatment and robotic training. *J Neurosci* 2005;25:11738–11747. [PubMed: 16354932]
- Glaum SR, Proudfit HK, Anderson EG. 5-HT<sub>3</sub> receptors modulate spinal nociceptive reflexes. *Brain Res* 1990;510:12–16. [PubMed: 2322835]
- Hains BC, Johnson KM, McAdoo DJ, Eaton MJ, Hulsebosch CE. Engraftment of serotonergic precursors enhances locomotor function and attenuates chronic central pain behavior following spinal hemisection injury in the rat. *Exp Neurol* 2001;171:361–378. [PubMed: 11573989]
- Hentall ID, Mesigil RP, Pinzon A, Noga BR. Temporal and spatial profiles of pontine-evoked monoamine release in the rat's spinal cord. *J Neurophysiol* 2003;89:2943–2951. [PubMed: 12612020]
- Hentall ID, Pinzon A, Noga BR. Spatial and temporal patterns of serotonin release in the rat's lumbar spinal cord following electrical stimulation of the nucleus raphe magnus. *Neuroscience* 2006;142:893–903. [PubMed: 16890366]
- Hochman, S.; Garraway, S.; Machacek, D.; Shay, B. 5-HT receptors and the neuromodulatory control of spinal cord function. In: Cope, T., editor. *Methods and New Frontiers in Neuroscience Series: Motor Neurobiology of the Spinal Cord*. Boca Raton, FL: CRC Press; 2001. p. 47-87.
- Jackson BP, Wightman RM. Dynamics of 5-hydroxytryptamine released from dopamine neurons in the caudate putamen of the rat. *Brain Res* 1995;674:163–166. [PubMed: 7773688]
- Kiehn O, Kjærulff O. Spatiotemporal characteristics of 5-HT and dopamine-induced rhythmic hindlimb activity in the in vitro neonatal rat. *J Neurophysiol* 1996;75:1472–1482. [PubMed: 8727391]
- Kjærulff O, Kiehn O. Distribution of networks generating and coordinating locomotor activity in the neonatal rat spinal cord in vitro: a lesion study. *J Neurosci* 1996;16:5777–5794. [PubMed: 8795632]
- Lopez-Garcia JA. Serotonergic modulation of the responses to excitatory amino acids of rat dorsal horn neurons in vitro: implications for somato-sensory transmission. *Eur J Neurosci* 1998;10:1341–1349. [PubMed: 9749788]
- Madden CJ, Morrison SF. Serotonin potentiates sympathetic responses evoked by spinal NMDA. *J Physiol* 2006;577:525–537. [PubMed: 16973701]

- Marinesco S, Poncet L, Debilly G, Jouvet M, Cespuglio R. Effects of tianeptine, sertraline and clomipramine on brain serotonin metabolism: a voltammetric approach in the rat. *Brain Res* 1996;736:82–90. [PubMed: 8930312]
- McLone DG, Bondareff W. Developmental morphology of the subarachnoid space and contiguous structures in the mouse. *Am J Anat* 1975;142:273–294. [PubMed: 1119412]
- Michael D, Travis ER, Wightman RM. Color images for fast-scan CV measurements in biological systems. *Anal Chem News Features* 1998:586A–592A.
- Montañez S, Daws LC, Gould GG, Frazer A. Serotonin (5-HT) transporter (SERT) function after graded destruction of serotonergic neurons. *J Neurochem* 2003;87:861–867. [PubMed: 14622117]
- Morse DE, Low FN. The fine structure of the pia mater in the rat. *Am J Anat* 1972;133:349–368. [PubMed: 5026660]
- Nicholson C, Syková E. Extracellular space structure revealed by diffusion analysis. *Trends Neurosci* 1998;21:207–215. [PubMed: 9610885]
- Noga BR, Pinzon A, Ballester B, Ospina D, Hentall ID. Serotonin concentrations in the adult rat spinal cord (SC) measured simultaneously by fast cyclic voltammetry (FCV) at several locations following microinjection or surface application. *Soc Neurosci Abstr* 2005;31:749.12.
- Noga BR, Pinzon A, Mesigil RP, Hentall ID. Steady-state levels of monoamines in the rat lumbar spinal cord: spatial mapping and the effect of acute spinal cord injury. *J Neurophysiol* 2004;92:567–577. [PubMed: 15014108]
- Phillips PEM, Stamford JA. Voltammogram “landscapes” aid detection of in vivo electrochemical signals. *Electroanalysis* 1999;11:301–307.
- Prokopová S, Vargová L, Syková E. Heterogeneous and anisotropic diffusion in the developing rat spinal cord. *Neuroreport* 1997;8:3527–3532. [PubMed: 9427320]
- Reina MA, Casasola ODL, Villanueva MC, López A, Machés F, Andrés JAD. Ultrastructural findings in human spinal pia mater in relation to subarachnoid anesthesia. *Anesth Analg* 2004;98:1479–1485. [PubMed: 15105235]
- Rice ME, Okada YC, Nicholson C. Anisotropic and heterogeneous diffusion in the turtle cerebellum: implications for volume transmission. *J Neurophysiol* 1993;70:2035–2044. [PubMed: 7507522]
- Schmauss C, Hammond DL, Ochi JW, Yaksh TL. Pharmacological antagonism of the antinociceptive effects of serotonin in the rat spinal cord. *Eur J Pharmacol* 1983;90:349–357. [PubMed: 6688398]
- Schmidt BJ, Jordan LM. The role of serotonin in reflex modulation and locomotor rhythm production in the mammalian spinal cord. *Brain Res Bull* 2000;53:689–710. [PubMed: 11165804]
- Šimonová Z, Svoboda J, Orkand R, Bernard CCA, Lassmann H, Syková E. Changes of extracellular space volume and tortuosity in the spinal cord of Lewis rats with experimental autoimmune encephalomyelitis. *Physiol Res* 1996;45:11–22. [PubMed: 8884919]
- Stamford, JA.; Crespi, F.; Marsden, CA. In vivo voltammetric methods for monitoring amine release and metabolism. In: Stamford, JA., editor. *Monitoring Neuronal Activity*. New York: Oxford Univ. Press; 1992. p. 113-145.
- Sur C, Betz H, Schloss P. Localization of the serotonin transporter in rat spinal cord. *Eur J Neurosci* 1996;8:2753–2757. [PubMed: 8996825]
- Syková E. Extrasynaptic volume transmission and diffusion parameters of the extracellular space. *Neuroscience* 2004;129:861–876. [PubMed: 15561404]
- Syková E, Chvátal A. Extracellular ionic and volume changes: the role in glia-neuron interaction. *J Chem Neuroanat* 1993;6:247–260. [PubMed: 8104419]
- Syková E, Mazel T, Vargová L, Voříšek I, Prokopová-Kubinová S. Extracellular space diffusion and pathological states. *Prog Brain Res* 2000;125:155–178. [PubMed: 11098655]
- Syková E, Svoboda J, Polák J, Chvátal A. Extracellular volume fraction and diffusion characteristics during progressive ischemia and terminal anoxia in the spinal cord of the rat. *J Cereb Blood Flow Metab* 1994;14:301–311. [PubMed: 8113325]
- Willis WD, Westlund KN. Neuroanatomy of the pain system and of the pathways that modulate pain. *J Clin Neurophysiol* 1997;14:2–31. [PubMed: 9013357]
- Xu W, Qiu XC, Han JS. Serotonin receptor subtypes in spinal antinociception in the rat. *J Pharmacol Exp Ther* 1994;269:1182–1189. [PubMed: 8014862]

- Zahniser NR, Dickinson SD, Gerhardt GA. High-speed chronoamperometric electrochemical measurements of dopamine clearance. *Methods Enzymol* 1998;296:708–719. [PubMed: 9779484]
- Zhou FC, Lesch K-P, Murphy D. Serotonin uptake into dopamine neurons via dopamine transporters: a compensatory alternative. *Brain Res* 2002;942:109–119. [PubMed: 12031859]

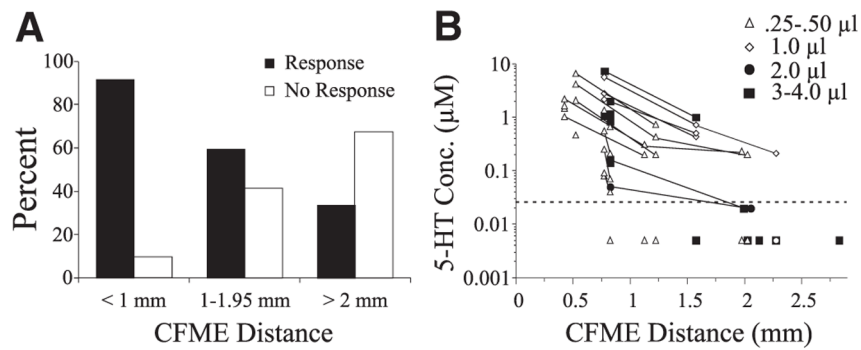
**FIG. 1.**

Postexperimental in vitro calibration of carbon fiber microelectrodes (CFMEs) with 5-hydroxytryptamine (5-HT; serotonin) and the 5-HT reuptake inhibitor clomipramine. **A:** triangular input waveform or scan indicating both the oxidation (Ox) and reduction (R) phases, subtracted voltammograms for different concentrations of 5-HT, full signals obtained before and after the addition of 5-HT (overlaid) illustrating current changes due to the oxidation and reduction of 5-HT, and a subtracted voltammogram for clomipramine, illustrating oxidation and reduction currents. Dashed line indicates where the peak oxidation of 5-HT typically occurs. Note double and single reduction peaks (arrowheads) for 5-HT and clomipramine, respectively. **B:** average oxidation currents ( $\pm$ SE) evoked by different concentrations of 5-HT for electrodes used in microinjection experiments. Note linearity of response. **C:** color raster plot of 5-HT obtained during a postexperimental calibration. Each individually subtracted voltammogram is positioned according to its acquisition time during the trial (scanned at 2 Hz). Current generated during each scan was color coded (scale illustrated on the *right*) to evaluate the evolving response to increasing concentrations of 5-HT. Raster plot illustrates selected regions of the voltammogram (as indicated in **A**: red and blue bars), with the *bottom half* of the plot showing oxidation currents (in yellow and red) and the *top half* of the plot showing corresponding reduction currents (in blue, purple, and black). Note that 5-HT evokes a single oxidation current and 2 postoxidation reduction currents, and that the oxidation peak widens and the reduction peaks deepen as the concentration is increased. **D:** color raster plot for differing concentrations of clomipramine. Note the single oxidation and reduction peaks.

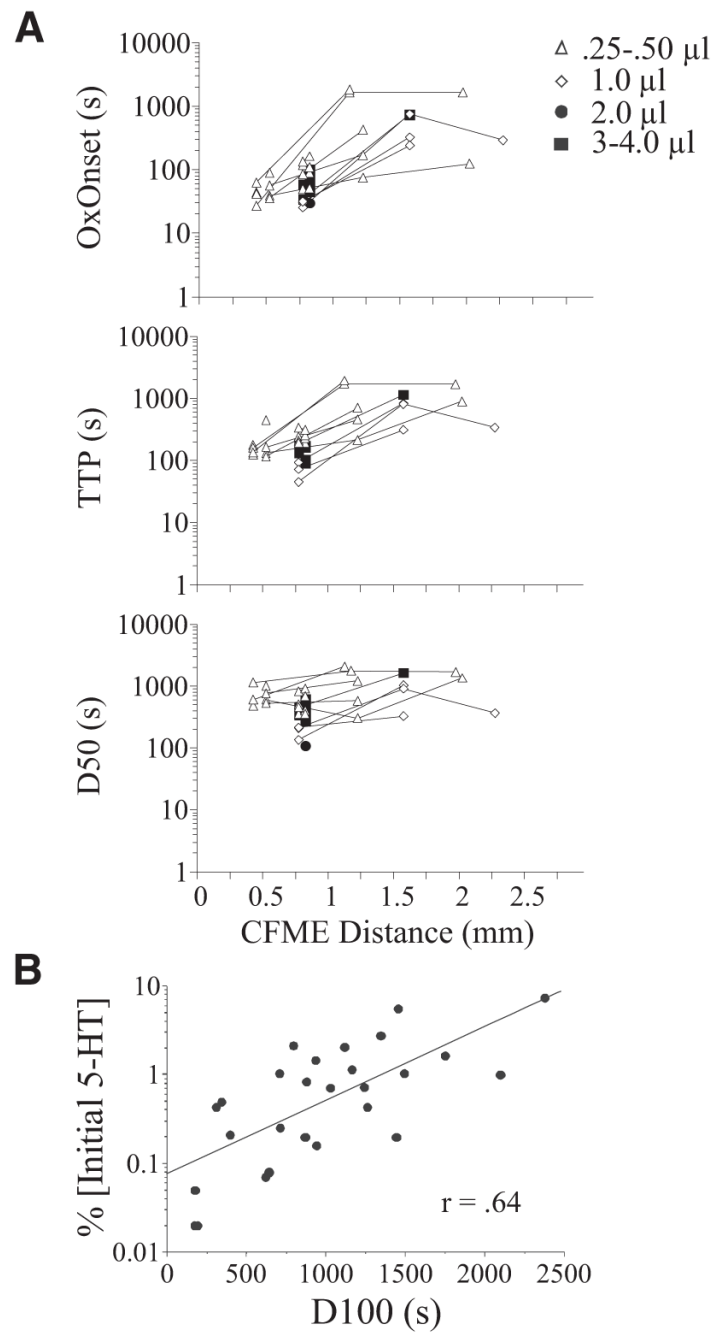


**FIG. 2.** Experimental trial of 5-HT microinjection into the spinal cord. *Left:* 2 CFMEs, e0 and e1 (yellow), and the 5-HT micropipette (red) were lowered into lamina IV of the L2 spinal segment. e0 was 500  $\mu\text{m}$  and e1 was 2,000  $\mu\text{m}$  away from the 5-HT micropipette. *Right:* color representations showing serotonergic redox signals at e0 and e1 after microinjection of 0.5  $\mu\text{l}$  (dashed line) of 100  $\mu\text{M}$  5-HT over 1 min. Note that 5-HT was detected sooner and at a much higher concentration by e0 compared with e1.

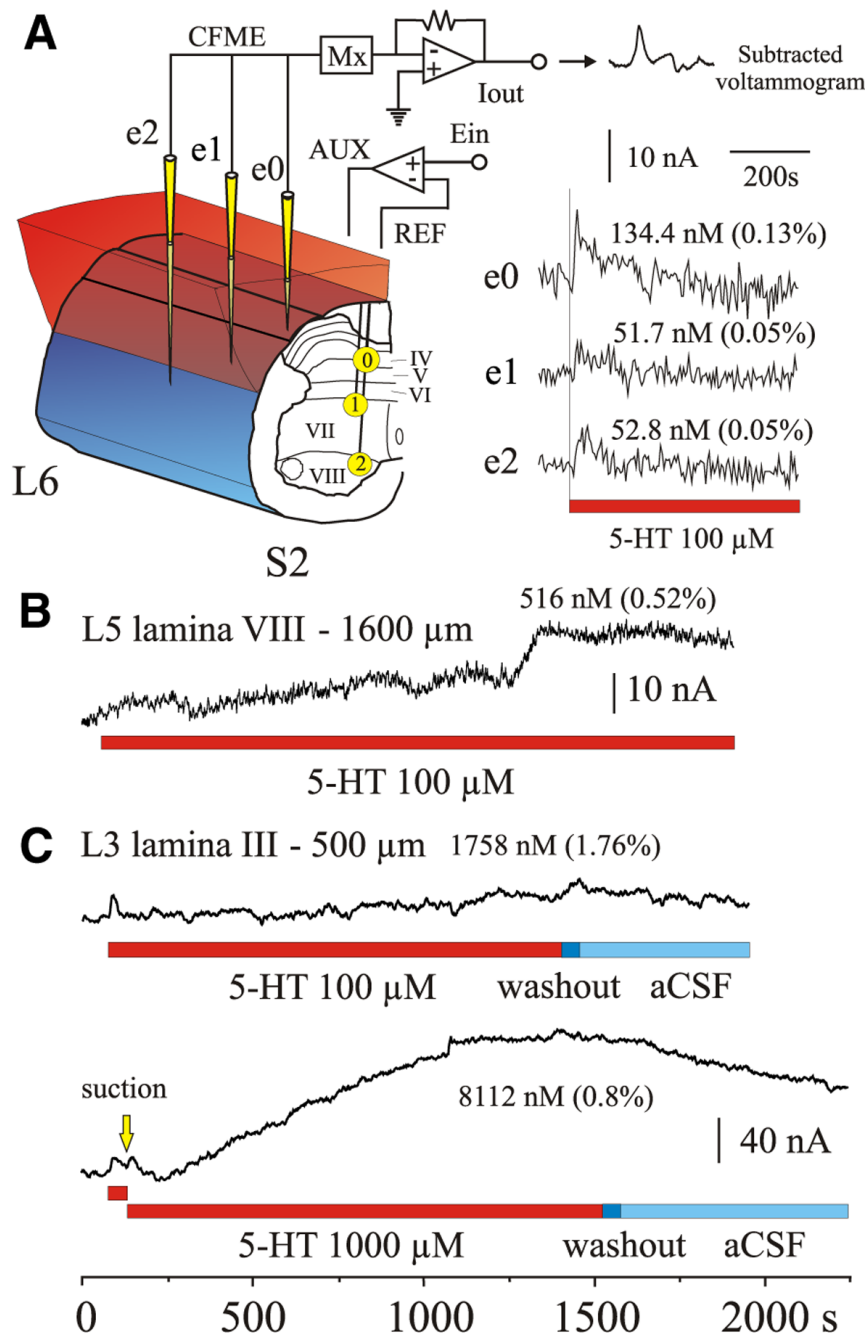


**FIG. 3.**

Spread of 5-HT ( $100 \mu\text{M}$ ) through the spinal cord measured at different distances from the site of microinjection. *A*: percentage of CFMEs that showed a 5-HT oxidation current (response vs. nonresponse). CFMEs were positioned <1 mm away (*Close*), between 1 and 2 mm away (*Intermediate*) or  $\geq 2$  mm away (*Far*) from the injection site. *B*: concentration of 5-HT detected as a function of distance. Symbols to the *right* denote volume of injected 5-HT (0.25– 4.0  $\mu\text{l}$ ). Responses of CFMEs during the same experimental trial are connected with a solid line. Note that the concentration diminishes rapidly with increasing distance. Observations below average detection threshold (dotted line) indicated at “0.005  $\mu\text{M}$ ” are included, providing that 5-HT was detected with other electrodes in the same trial.

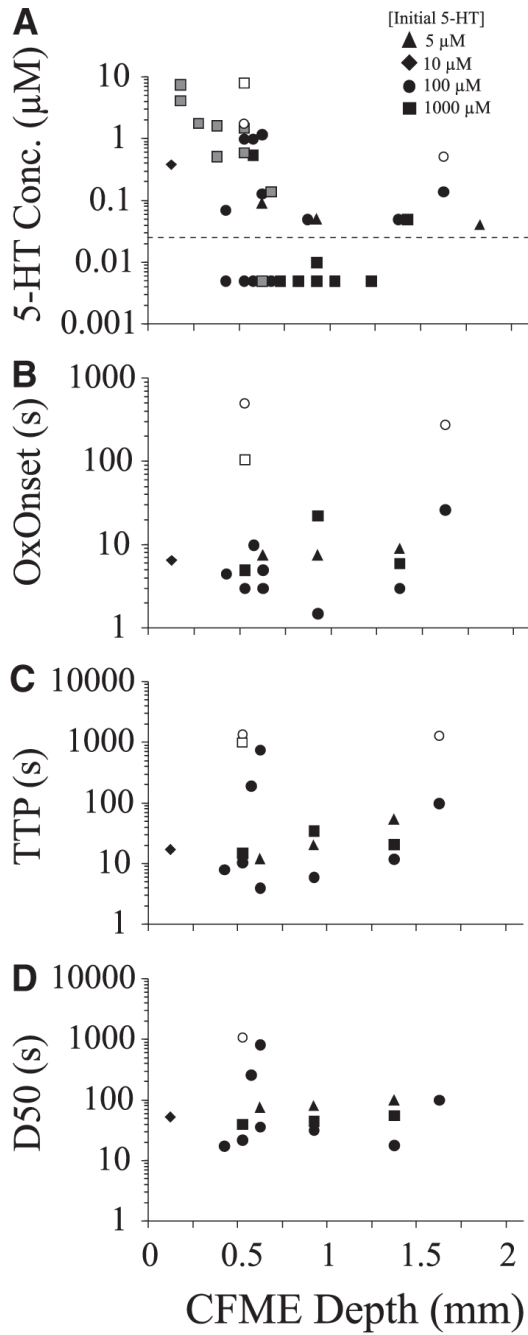


**FIG. 4.** Diffusion parameters of 5-HT within the spinal cord after microinjection (100  $\mu$ M). *A*: relationships between oxidation onset (OxOnset), time-to-peak (TTP), and latency to 50% decay ( $D_{50}$ ) of 5-HT oxidation current and distance from site of microinjection of 5-HT. Symbols to the *right* denote volume injected (0.25–4.0  $\mu$ l). *B*: positive relationship between 5-HT concentration (% initial 5-HT) and latency to 100% decay ( $D_{100}$ ) of 5-HT oxidation current ( $r = 0.64$ ).



**FIG. 5.** 5-HT superfusion of the dorsal surface of the spinal cord. *A, left:* 3 CFMEs (yellow) were positioned in caudal spinal segments L6, S1, and S2. Electrodes were placed into laminae IV (e0), VII (e1), and VIII (e2). Shortest distance from the CFME tip to the spinal cord surface exposed by the laminectomy was 600, 900, and 1,350 μm for e0, e1, and e2, respectively. *Right:* shortly after application of 100 μM 5-HT, concentrations increased within the spinal cord as determined by oxidation of 5-HT at all CFMEs (see sample voltammogram). Peak oxidation current amplitude is plotted for each electrode. This early response peaked within 4–12 s of application and gradually returned to baseline. Maximum concentrations and percentage of applied 5-HT concentration are indicated. Time of exposure to 5-HT in all panels

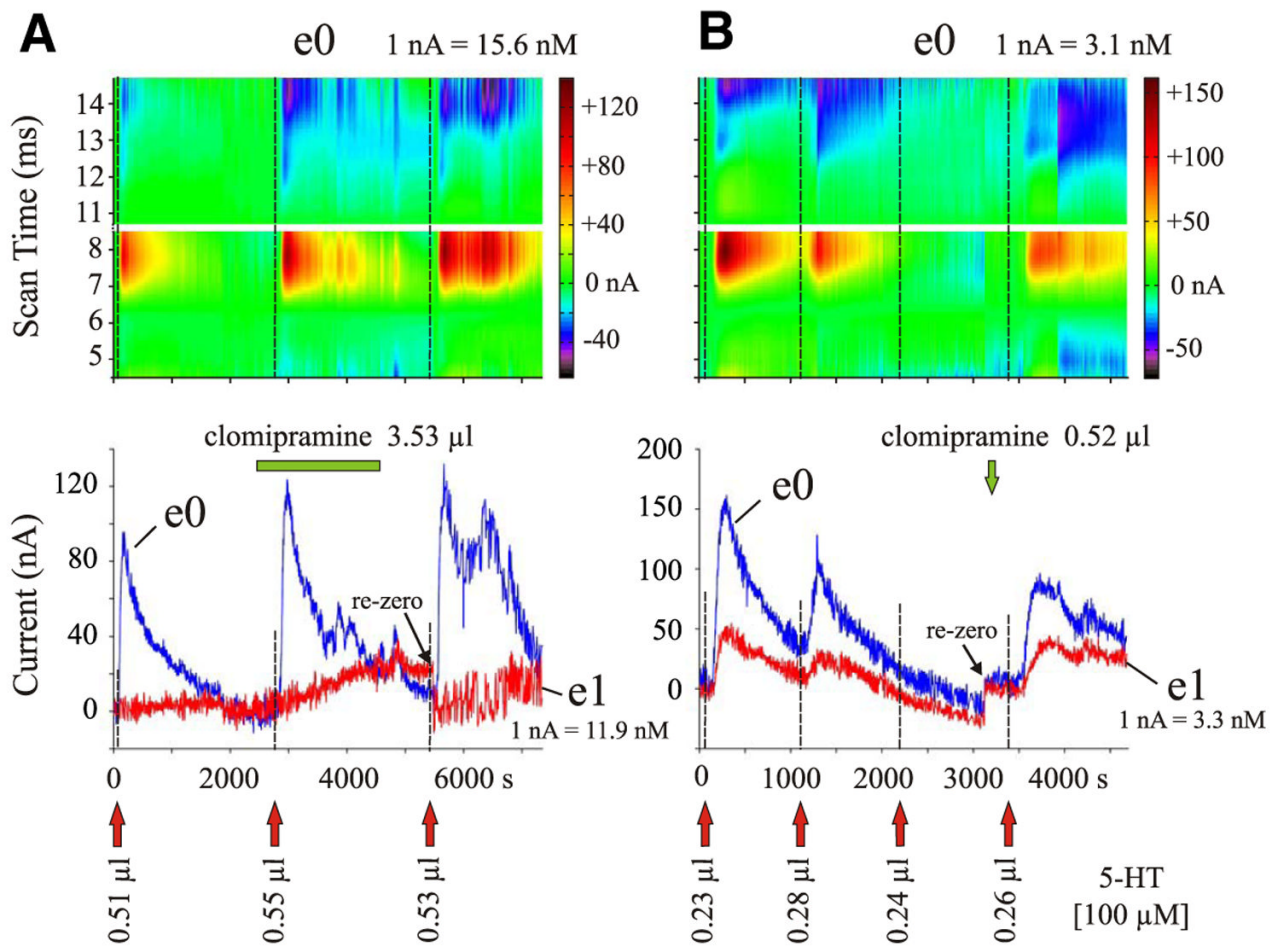
is indicated by the *red bar*. *B* and *C*: peak oxidation current amplitude plots from 2 other experiments illustrating changes in 5-HT concentration (both early and late responses) to superfusion with either 100 or/and 1,000  $\mu\text{M}$  5-HT. Note the gradual increase in concentration with time after the initial response. A drop in concentration (*C*) was observed after washout. Washout of 5-HT is indicated by dark blue bar; artificial cerebrospinal fluid (aCSF) bathing medium indicated by light blue bar. Locations and electrode depth (from closest exposed surface area) are indicated, as is the peak concentration of 5-HT for the late response. *Bottom trace* shows that the early response could be reproduced with a second application of 5-HT [removed by suction (yellow arrow) between applications].



**FIG. 6.** Response of CFMEs placed at various depths within the spinal cord to bath superfusion of 5-HT. Concentration detected (A), OxOnset (B), TTP (C), and D<sub>50</sub> (D) are plotted relative to CFME depth from the closest exposed surface of the spinal cord. Symbols to the right denote concentration of applied 5-HT (5–1,000  $\mu\text{M}$ ). Closed symbols denote initial (early) responses; open symbols denote second (late) responses. For concentration detected, observations below average detection threshold (dotted line) indicated at “0.005  $\mu\text{M}$ ” are included, providing that 5-HT was detected with other electrodes in the same trial. In one experiment, electrodes in ventral locations were repositioned to more dorsal locations to obtain concentration



measurements (gray symbols) and it was not known whether the values were from an early or late response.

**FIG. 7.**

5-HT peak oxidation currents of individual CFMEs before and after microinjection of clomipramine. **A:** 5-HT concentrations were measured with 2 electrodes, located 400  $\mu$ m away ( $e_0$ ) and 1,150  $\mu$ m away ( $e_1$ ) from the 5-HT and clomipramine micropipettes, in lamina III of spinal segment L6. *Top:* color raster plots of 5-HT redox currents for  $e_0$ . *Bottom:* plot shows maximum peak oxidation currents for both electrodes. Microinjection of 3.53  $\mu$ l clomipramine (100  $\mu$ M) was preceded by one and followed by 2 separate 5-HT microinjections. Red arrows indicate when 5-HT (100  $\mu$ M) was microinjected (0.50  $\mu$ l/min each); the green bar indicates time of clomipramine application (0.1  $\mu$ l/min). Note increase in amplitude and prolongation of response to 5-HT after clomipramine. **B:** microinjection of 0.52  $\mu$ l clomipramine (10  $\mu$ M, 0.5  $\mu$ l/min; green arrow) preceded by 3 and followed by one 5-HT microinjection (100  $\mu$ M, 0.25  $\mu$ l/min; red arrows). In this experiment, CFMEs were located 750  $\mu$ m away ( $e_0$ ) and 834  $\mu$ m away ( $e_1$ ) from the 5-HT micropipette (located between the CFMEs in a fixed array), in lamina V of spinal segment L2. Clomipramine ejection electrode was positioned 400  $\mu$ m away from  $e_0$  and 1,950  $\mu$ m away from  $e_1$ . Plots as in A. Repeated 5-HT microinjections given in close succession showed diminishing responses that were reinstated with administration of clomipramine.